

Polymer MEMS Actuators for Underwater Micromanipulation

Jennifer W. L. Zhou, Ho-Yin Chan, Tony K. H. To, King W. C. Lai, and Wen J. Li, *Member, IEEE*

Abstract—Conventional MEMS actuators are not suitable for underwater applications such as cell grasping due to two main reasons: 1) their required actuation voltage are typically higher than 2 V, which would cause electrolysis in water and 2) they have small displacement/deflection due to their inherent driving principles. In this paper, three-different types of novel polymer-based MEMS underwater actuators developed in our laboratory are discussed: 1) ionic conducting polymer films (ICPF) actuator, which actuates by stress gradient induced by ionic movement due to electric field; 2) parylene thermal actuator, which actuates due to the induced stress gradient across a structure made of different layers of materials with different thermal expansion coefficients; and 3) polyaniline (PANI) actuator, which actuates due to its volumetric change caused by a reversible electrochemical oxidation-reduction (redox) reaction. All these polymer micro actuators can be actuated underwater with large deflections and require less power input than conventional MEMS actuators. The experimental results from characterizing these prototype actuators are presented in this paper.

Index Terms—Cellular grippers, micro manipulation, micro polymer actuators, polymer MEMS actuators.

I. INTRODUCTION

POTENTIAL applications for microrobotics with growing interest are cell manipulation, cell isolation, and micro injection (e.g., see [1]). For example, biologists usually use pipettes for cell isolation prior to carrying out micro injection. However, the functionality of this method is limited by the size of the cells, i.e., the cells cannot be too small compared to the pipette; otherwise, a bundle of cells could be drawn into the pipette at once. In addition, the pipette cannot be used to rotate individual cells, a function which is highly desirable during a micro injection process. To address these problems, we are currently developing an on-chip microrobotic gripper system that can eventually be used to manipulate and isolate cells controllably and enable localized cell probing and measurement. We report in this paper several novel micro polymer-based actuators that can be configured to form single-finger or multiple-finger underwater robotic grippers for cell grasping and manipulation.

Manuscript received June 10, 2003; revised March 1, 2004. This work is supported in part by the Hong Kong Research Grants Council (CUHK4206/00E), in part by the Chinese Academy of Sciences Distinguished Overseas Scholar Grant, and in part by the Chinese National High Technology Research and Development under grant (863) Plan (No. 2002AA431620).

J. W. L. Zhou, H. Y. Chan, T. K. H. To, and K. W. C. Lai are with the Center for Micro and Nano Systems, The Chinese University of Hong Kong, Shatin, Hong Kong.

Wen J. Li is with the Center for Micro and Nano Systems, The Chinese University of Hong Kong, Shatin, Hong Kong, he is also with the Micro and Nano Automation Laboratory, Shenyang Institute of Automation, Chinese Academy of Sciences, Shenyang, Liaoning, China.

Digital Object Identifier 10.1109/TMECH.2004.828652

Although many MEMS actuators exist already they are all hindered by one or more of the following factors when actuation in biological fluids is required: small displacement, small force output, large power consumption, large voltage requirement, and bioincompatibility. For example, electrostatic actuators are inefficient in ion-rich fluid and their deflection is very small [2]. Therefore, thermal actuators were considered by some researchers to operate in solution-based environments. Thermal actuators generally consist two structural layers with different thermal expansion coefficients ("bimorph"). One of the layers would be used as a heater to generate heat to induce thermal expansion of the two layers. Due to mismatch of the thermally-induced strain, the structure could be made to bend as a function of the heat generated. Even though thermal actuators can produce larger force and deflection than other types of MEMS actuators, they require higher power to actuate. G. Lin *et al.* [3] demonstrated a two-layer thermal actuator ($200 \times 45 \times 1.1 \mu\text{m}$ with polyimide/Au layers) that can operate in air with 7 V at 4 mA. However, to operate in liquid, it required over 100 V to actuate and overheated the actuator. M. Ataka *et al.* [4] also fabricated a thermal bimorph actuator ($500 \times 100 \times 6 \mu\text{m}$ with polyimide/Au layers) which rose up to 260°C for actuation in water—a temperature that would definitely kill cells. Recently, researchers have begun to look into other materials and mechanisms for underwater actuation. For example, Jager *et al.* [5] and Smela *et al.* [6] have pioneered the usage of polypyrrole polymers to fabricate micro aqueous actuators that can be driven under 2 V. However, their actuators are limited to operation in electrolyte solutions, which are not suitable for the survival of many biological entities.

II. ESTIMATION OF REQUIRED ACTUATION FORCE

Actuation in air and in water is very different physically. Hence, an estimate of the required force to actuate an actuator should be carried out to find the required force to deflect a structure in a liquid medium. The minimum force output of an underwater actuator must exceed the sum of the *fluid drag*, *gravitational* (weight) and the *spring restoring force* (bending stress force) in order for it to actuate and grip a cell. Note that in a liquid medium, *capillary force* (a surface force) between the actuator and the substrate is not a concern because of the absence of air-liquid interface, which may only exist for actuators operating in air. Possible forces of interaction for a micro actuator are depicted in Fig. 1.

As we have shown in [7], the most important force to overcome for an actuator in water is the spring restoring force, which depends on the structural material(s) used to make the actuator. This force can be estimated using the linear bending beam

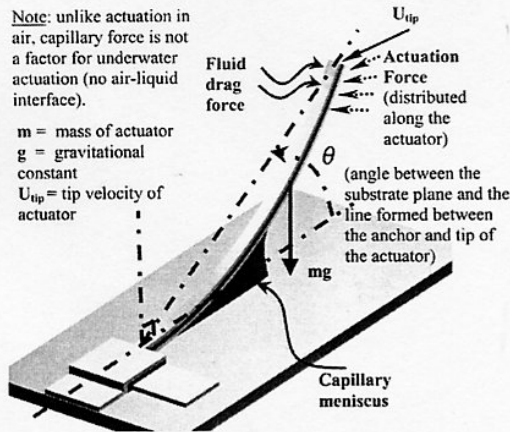


Fig. 1. Illustration showing various forces acting on an actuator operating in a fluidic medium. Note that in a liquid medium, buoyancy force may also be a factor.

TABLE I
 SPRING RESTORING FORCE FOR VARIOUS TYPES OF ACTUATORS (DIMENSION OF ACTUATOR: WIDTH = 100 μm, THICKNESS = 1 μm, LENGTH = 2 mm, FULL DEFLECTION = 1.27mm). ALL MATERIAL DATA WERE OBTAINED FROM [9], UNLESS OTHERWISE SPECIFIED

Types of Actuator	Weight (nN) $g=9.81m/s^2$	Flexura l rigidity 'EI' (pNm ²)	Density (kg/m ³)	Spring Restoring Force (nN)
Single Crystal Silicon	4.75	1.35	2420	644.58
Polysilicon	4.57	1.42	2330	676.41
Silicon Dioxide	5.22	0.62	2660	294.44
Silicon Nitride	6.75	1.29	3440	616.73
Gold (Au)	38.06	0.67	19400	318.31
Platinum (Pt)	42.18	1.23	21500	584.90
Parylene C*	2.53	0.03	1289	12.73
Nafion	3.87	0.002	1970	0.80
Parylene/Pt/Parylene Composite (.2/.6/.2)	26.32	0.29	~ same as Pt	128.69
Au/Nafion/Au Composite (.2/.6/.2)	17.5	0.52	~ same as Au	247.01
A 10um diameter air bubble in water	5.1pN (buoyancy force)	Not applicable	Not applicable	Not applicable

*Material properties of parylene product from Cookson Electronics [10]

theory. The actuation force required to deform a beam with a spring constant $k = 3E(wt^3/12)/l^3$ by a distance y is approximated by $F_k = ky$. This is the force produced by the induced stress of the beam by diversified principles. For a multiplayer structure, the product of Young's modulus E and inertia I must be defined with respect to the torque neutral axis (e.g., see [8]). The spring restoring force for actuators made of several different materials is tabulated and given in Table I, which shows that the spring restoring force for common MEMS materials is much higher than the gravitation force (weight) of the actuator. The equations to approximate the fluid drag force are provided in [7]. Referring to that publication, we have concluded that the spring restoring force is much more significant than the fluid drag force and buoyancy force for an actuator operating in a

TABLE II
 COMPARISON OF PHYSICAL PROPERTIES OF VARIOUS MEMS THIN FILM MATERIALS

	Coefficient of thermal expansion [K ⁻¹]	Density [kgm ⁻³]	Young's Modulus [G Pa]	Thermal Conductivity [Wm ⁻¹ K ⁻¹]
Platinum [9]	9×10^{-6}	2145	146.9	69.23
Polysilicon [9]	2.5×10^{-6}	2300	170	28
SiO ₂ [9]	12×10^{-6}	2300	83	1.38
Parylene C*	3.5×10^{-3}	1289	3.2	0.082
Nafion	Not Available	1970**	0.2	Not Available
PANI	--	1329	2	0.01

*Material properties of parylene product from Cookson Electronics [10]

** Material properties from Dupont Co.[12]

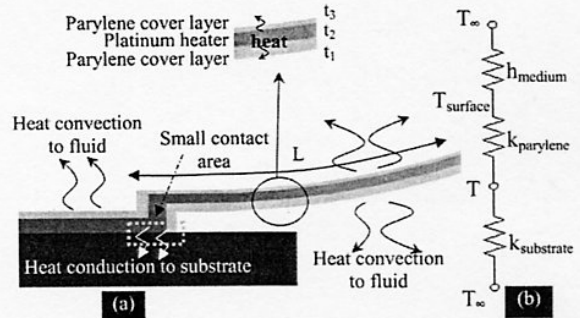


Fig. 2. (a) Illustration showing the cross-section of the thermal actuator; the heat transfer mechanisms of the actuator are also shown. (b) The corresponding equivalent heat-transfer circuit.

liquid medium. The spring restoring force for several MEMS materials and the polymer materials used in our current investigation are tabulated in Table I. As indicated, a minimal force in the order of a few hundred nano-Newtons must be generated by whichever means of actuation mechanism necessary in order to deflect a 2 mm × 100 μm × 1 μm structure in water.

III. PARYLENE THERMAL ACTUATOR

Conventional MEMS thermal actuators require relatively high actuation power in aqueous media because much of the input power is dissipated in the form of heat by: 1) conduction to the substrate by the small contact area between the substrate and the actuator (anchor), and 2) convection to the surrounding fluid environment (see Fig. 1). For the anchor, since the conduction path to the substrate is very short, i.e., a few microns of thin film thickness, thus, the heat conduction rate becomes faster and more energy input required. In addition, for actuation in aqueous environment, heat loss to liquid is much greater than that to the air, e.g., the convective heat coefficient of water is ~40 times higher than that of air. Our ongoing work is to use parylene C as a thin film polymer to encapsulate a thin film metal heater, resulting in a trilayered thermal actuator. Parylene C is biocompatible, has excellent thermal and electrical insulation properties, and has a much large coefficient of thermal expansion (CTE) than typical metals (see Table II). All these factors make parylene C a much more ideal material for creating large-deflection and low-power underwater actuators than typical MEMS thin film materials such as SiO₂, Si₃N₄,

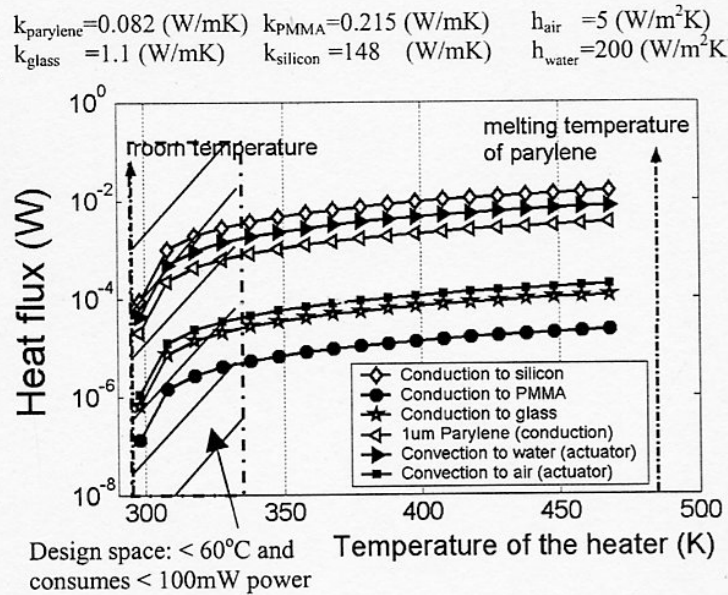


Fig. 3. Comparison of heat loss of the actuator through conduction for various substrate materials and through convection to air and water.

and polysilicon. However, the drawback is that parylene C melts at $\sim 180^\circ\text{C}$, which is a much lower temperature than for most common MEMS materials. Hence, a key part of our project was to develop a micro fabrication process to realize the trilayer thermal actuator structure using parylene C.

A. Comparison of Heat Dissipation in Water and in Air

By applying the energy balance equation for heat generation and transfer [11] on the platinum metal heater [refer to the equivalent thermal circuit in Fig. 2(b)] the following can be derived:

$$\rho C_p V \frac{\partial T}{\partial t} = I^2 R - \left[\frac{(B_{\text{parlylene}}/k_{\text{parlylene}}) + (1/h_{\text{medium}}) A_{\text{convection}}}{B_{\text{substrate}}/k_{\text{substrate}}} A_{\text{conduction}} \right] (T - T_\infty) \quad (1)$$

where B is the thickness, k is the thermal conductivity, h is the convection heat transfer coefficient, ρ is the density, C_p is the specific heat capacity, A is the effective area for heat loss, and T is the temperature of the heater. Using the above equation, a comparison of heat loss through convection in water and air and conduction through an actuator's anchor for various substrate materials is given in Fig. 3.

As shown, the convection heat loss in water is almost two orders of magnitude higher than in air and, therefore, minimizing the convection to aqueous environment is important in minimizing a thermal actuator's energy consumption. By using parylene, which has lower thermal conduction than other standard MEMS insulators, convection loss can be reduced. However, as shown in the figure, the most significant heat loss is by conduction to the Si substrate through the small anchor area. Nevertheless, the graph also indicates that the trilayer parylene actuators may function at 60°C with total power consumption of <100 mW (design space). This power loss is comparable to

many reported MEMS underwater actuators while allowing this polymer actuator to operate at a much lower temperature.

B. Temperature-Induced Deflection for a Trilayer Thermal Actuator

The deflection of this polymer-based thermal actuator as a function of temperature can be estimated by a three-layer cantilever beam model. The basic actuator structure consists of a middle layer of platinum and top and bottom layers of parylene. When an electrical current is passed through the platinum heater, the entire structure will expand. Due to the difference in CTE between platinum and parylene, different strains will be developed in the three layers and, thereby, lead to the curling up of the beam if the thicknesses of the layers are designed appropriately. By considering the interaction of forces and moments between the layers, the bending radius of curvature r due to temperature change ΔT can be calculated by the following:

$$r = g(E_i, I_i, \alpha_i, w_i) / \Delta T. \quad (2)$$

The subscript i is the parameter for the i th layer. In the above equations, α, t, w, E , and I are the CTE, thickness, width, Young's modulus and moment of inertia of the corresponding layers, respectively. For the exact function of $g(E_i, I_i, \alpha_i, w_i)$, refer to [7].

From (2), the bending radius is inversely proportional to temperature change. We set $\Delta T = 40^\circ\text{C}$ as the maximum allowable temperature change in designing the actuators (biological cells may still survive at 40°C above room temperature). In order to minimize the radius of curvature of the trilayer beam given a ΔT , the function $g(E_i, I_i, \alpha_i, w_i)$ should be minimized. A detail description on the minimization method is given in [7]. If an actuator has dimensions $l = 2$ mm, $w_1 = w_2 = 100$ μm , $t_1 = .1$ μm , $t_2 = .2$ μm , and $t_3 = .3$ μm , then r of 600 μm can be achieved at $\Delta T = 40^\circ\text{C}$.

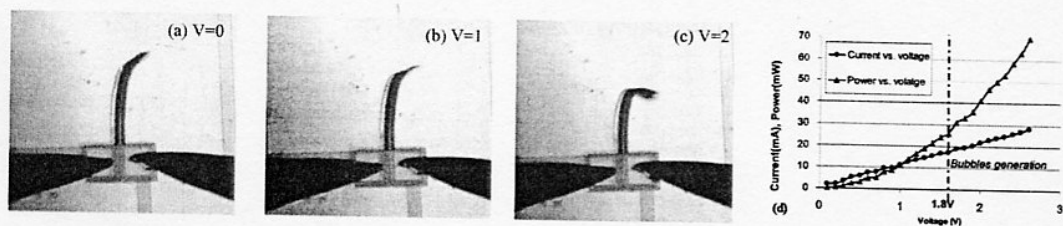


Fig. 4. Sequence of images showing the motion of an underwater actuator driven by applying a voltage. The $I - V$ relationship and power consumption for this actuator is shown in (d). The power consumption of ~ 60 mW at 2.5 V input was needed to achieve 90° deflection.

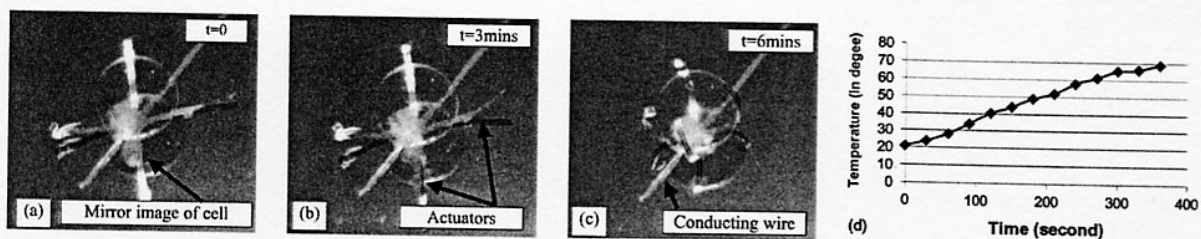


Fig. 5. Sequence of images showing the motion of an underwater actuator by increasing the water medium temperature from 23°C to 70°C . The captured object was a crab's egg with diameter ~ 1 mm.

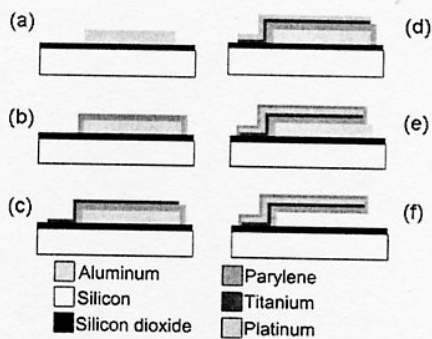


Fig. 6. Fabrication process of the polymer-based thermal actuator.

The fabrication process for the trilayer thermal actuator using parylene is provided in Fig. 6. Detailed description of the process flow is given in [7].

C. Experimental Results

There are two methods to induce a temperature change in the thermal actuators: 1) passing a current through the resistive heater to increase actuator temperature and 2) changing the temperature of the medium which surrounds the actuators to heat them up.

1) *Actuation by Applied Voltage:* A sequence of motion of a thermal actuator actuated underwater by an applied voltage is shown in Fig. 4. The experiment was carried out in distilled water. The resistance of the platinum heater was measured to be $\sim 90 \Omega$. The dimension of the actuator shown is $2 \text{ mm} \times 100 \mu\text{m} \times 0.6 \mu\text{m}$. The voltage was varied from 0 to 3 V (power input of ~ 100 mW at 3 V). It was found that bubbles were generated when the applied voltage was greater than 1.8 V (electrolysis); but we have found that by depositing parylene on metal surfaces, the number of bubbles that are generated by electrolysis can be significantly reduced. Experimentally, we have driven the thermal actuators with square wave input and

TABLE III
ACTUATOR PARAMETERS

Types of actuator	Parylene	Nafion	PANI	Poly-Si
Size of actuator	$l=2\text{mm}$ $w=100\mu\text{m}$ $t=0.6\mu\text{m}$	$l=1.2\text{mm}$ $w=100\mu\text{m}$ $t=0.4\mu\text{m}$	$l=2.5\text{mm}$ $w=500\mu\text{m}$ $t=1\mu\text{m}$	$l=2\text{mm}$ $w=100\mu\text{m}$ $t=0.6\mu\text{m}$
Fluidic drag force (speed dependent)	13.7nN	0.01nN	9.6nN	13.7nN
Spring-restoring force	0.2nN	32nN	27nN	3.44nN
Weight of actuator	8.44nN	5.1nN	16.5nN	2.76nN
Buoyancy force	1.2nN	0.48nN	12.3nN	1.2nN
Minimum actuation force	16.49nN	36.6nN	65.4nN	21.1nN
Voltage/Power requirement	100mW	7V	2.5 V	$> 7\text{V}$ $> 100\text{mW}$

observed that they can be fully actuated up to 3 Hz in liquid medium with full deflection. More extensive measurements on the frequency response of the actuators are ongoing in our lab.

2) *Actuation by Heating Fluidic Environment:* For actuation by increasing the fluidic medium temperature, the experiment was also carried out in DI water. The temperature of the water was raised from 23°C to around 60°C by a hotplate. *Danio rerio* follicles with diameters ranging from $500 \mu\text{m}$ to 1 mm were captured using this actuation method. We have also developed a multifinger gripper for demonstrating cell grasping as shown in Fig. 5. An advantage of using this actuation technique is that only external thermal energy needs to be applied to the medium, and therefore the actuators can be actuated without electrolysis. Full characterization on the performance of this polymer actuator is underway in our lab. The estimated actuation force of this actuator is given in Table III.

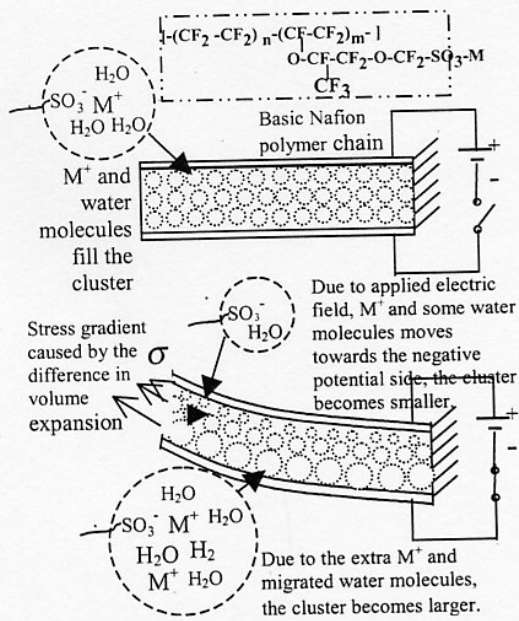


Fig. 7. (a) The chemical composition of Nafion. (b) A schematic drawing illustrating the principle of the electrically controllable bending of a metal/Nafion/metal sandwich structure.

IV. NAFION IONIC CONDUCTION ACTUATORS

In recent years, novel materials belonging to the electroactive polymers, such as Nafion-based Ionic Conducting Polymer Films (ICPF), polypyrrole or conjugated polymers, and PANI of conductive polymers, were investigated by researchers as possible artificial muscles [13]. These polymers offer the potential to break some of the limitations that are set by current MEMS thin film materials such as polysilicon, Si_3N_4 , and metals in engineering micro sensors and actuators. As mentioned in I, Smela and Jager *et al.* have developed fabrication processes for conjugated polymers and demonstrated micro-robotic appendages capable of manipulating micro objects in aqueous environments [13], [14]. Nevertheless, their actuators have slow response and were limited to operations in electrolyte solutions, which may not be suitable for the survival of many biological entities.

Our ongoing work is to investigate the possibility of using ionic conducting polymer to develop ICPF micro actuators. Nafion polymer tends to aggregate to form tightly packed regions referred to as clusters (see Fig. 7). Under an electric field, ions move in and out of the conducting polymers, which lead to simultaneous changes in volume as well as variations in physical properties. These polymers are undergoing intense analyses and improvements by the artificial muscles community. However, most of the reported ICPF actuators were developed using commercial Nafion membranes with standard thickness of $200 \mu m$. This film thickness restricts the allowable deflection of ICPF actuators when they are scaled down in length and width. In our previous work, ICPF actuators made from commercial Nafion 117 membrane were successfully fabricated using a Nd:YAG laser system [15]. Actuators with dimensions of $w = 300 \mu m$, $l = 3000 \mu m$, $t = 200 \mu m$ were actuated under water with 15 V DC voltage. Our current goal

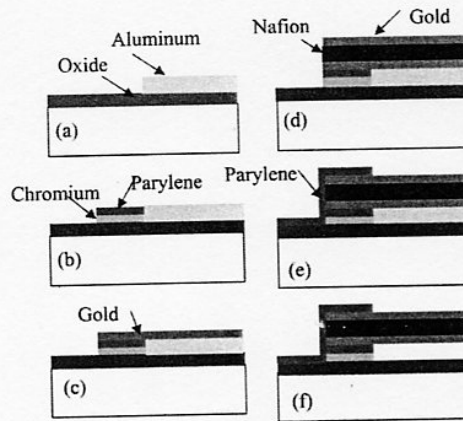


Fig. 8. Illustration of the Nafion actuator fabrication process steps. (a) Deposition and etching of sacrificial aluminum on oxidized Si. (b) Deposition and etching of adhesion promoting chromium layer; parylene coated and patterned. (c) Deposition and liftoff of bottom gold layer. (d) Deposition of Nafion by spin-on; deposition and etching of top gold layer; etching of Nafion by plasma. (e) Waterproof parylene layer coated and patterned. (f) Removal of sacrificial layer.

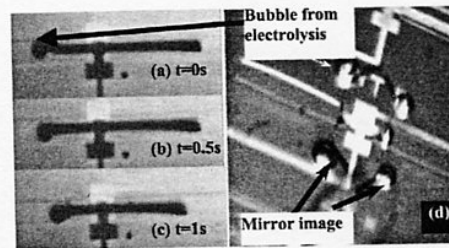


Fig. 9. A micro Nafion actuator under 5 V and 7 V DC voltage input. (a), (b), (c) are 2-D top views under 5 V. (d) is a 3-D picture of actuator under 7 V to reach full closure of gripper. The bubbles were caused by electrolysis of the aqueous medium.

is to find how well does the ionic conduction mechanism scale with size, i.e., if the relative large force to input voltage ratio and fast frequency response of ICPF actuation characteristics can be preserved at micro scale, then these actuators will find many new applications in the bio-manipulation area not accessible by existing MEMS actuators.

A. Fabrication of MEMS Nafion ICPF Actuators

Commercial Nafion solution from Dupont (SE-5012) was used to fabricate the ICPF micro actuators made of Au/Nafion/Au layers with the Nafion film thickness controlled by spin-on process. The major difficulty in this work was to develop a process to spin-on Nafion thin films to create MEMS structures. This task was successfully accomplished by a specialized spun-on-and-cured process as described in [17]. The process flow is shown in Fig. 8. In order to generate a relatively uniform thin film, we used $\sim 0.2 \mu m$ thick Nafion and $\sim 0.1 \mu m$ thick gold layers as electrodes in our process.

B. Experimental Results

The testing of the Nafion actuators was carried out using a micro probe station. A sequence of motion of a 2-finger actuator actuated in DI water is shown in Fig. 9 (2-D top-view

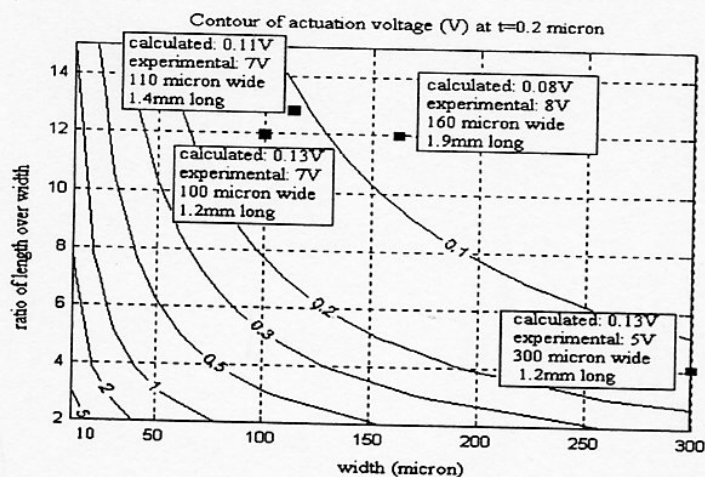


Fig. 10. Contour plots showing isolines of theoretical actuation voltages for Nafion actuators with various dimensions constructed by spin-on Nafion film (using $m_e = 37.5 \text{ Nm/Vm}^2$). The black dots show the dimensions with experimental actuation data.

under microscope). The actuator (each finger $w = 100 \mu\text{m}$, $l = 1200 \mu\text{m}$, $t = 0.4 \mu\text{m}$) started to deflect at $\sim 5 \text{ V}$. It reached full deflection, i.e., 90° change of tip direction when the voltage was $\sim 7 \text{ V}$. Gas bubbles due to electrolysis were generated from both electrodes. After the voltage was removed, the beams returned to their original positions. Input I-V characteristics of some actuators were obtained showing the power consumption of these micro ICPF actuators to be in the order of 50 mW (for a single finger structure with $w = 300 \mu\text{m}$, $l = 1200 \mu\text{m}$, and $t = 0.4 \mu\text{m}$).

Full characterization on the performance of the micro Nafion actuators is underway in our lab. The estimated actuation force and considerations on the actuation voltage of these underwater actuators are discussed below.

C. Size-Effect on Actuation Voltage

Several models have been reported to characterize the actuation behavior of commercial ICPF actuators [16]–[20]. Among them, the model proposed by Nemat-Nasser and Li [20] is the most comprehensive and revealed a relationship between the microstructural composition of the Nafion polymer. Effects from the ion type, cluster size, water transportation, electric field, and elastic deformation were all considered. Their results implied a direct relationship between the performance and dimensions of an actuator.

Here we compare Nemat-Nasser and Li's model to our experimental data in order to see if the dimensional scaling effect is valid. The voltage required for an actuator to reach full deflection is considered. To achieve a static deflection, the equivalent moment M_e induced by voltage is balanced by the bending moment M_k calculated by the conventional linear bending theory related to bending curvature. The induced moment in an actuator can be simplified as in (3), where κ_e is the effective dielectric constant of the polymer, ϕ_0 is the voltage applied, and a is a parameter approximately determined by electro-chemical parameters (see [20] for detail)

$$M_e = k_0 \kappa_e \phi_0 a t w. \quad (3)$$

Now, let m_e be an electromechanical coefficient, where $m_e = k_0 \kappa_e a$ (unit: Nm/Vm^2), which is also a parameter determined by the microstructural composition of the material and can be physically related to the moment induced by unit cross-sectional area of a Nafion film by unit voltage when ideally the electrical energy is completely converted into mechanical energy. Then the required actuation voltage for full deflection can be expressed as

$$\phi_0 = \pi EI / (m_e t l / w). \quad (4)$$

We have found that (4) predicts experimental results reasonably well for Nafion films of 50 to 200 microns thick. However, as the Nafion films decrease in thickness, the above equation does not agree well with experimental results. For instance, the theoretical voltage-dimension relationship for $0.2 \mu\text{m}$ thickness is shown in Fig. 10. It gives a guideline to the Nafion actuator structural design. That is, a family of geometric configurations on the contours can be found when an actuator is expected to achieve a full grasping motion with a given actuation voltage. In addition, for a given thickness, the contour is also a boundary for dimension selection. As shown, to achieve full closure of an actuator under 2 V , the width of the actuator should not be less than $40 \mu\text{m}$, with l/w ratio of 2 (or $10 \mu\text{m}$ width with l/w ratio of 8). Hence, the minimum diameter of cell that can be enclosed by a Nafion actuator should be $\sim 50 \mu\text{m}$ if the film can be reduced to $0.2 \mu\text{m}$. However, our experimental result as reported in the preceding section shows the actual voltage for actuators $100 \mu\text{m}$ wide, $\sim 0.2 \mu\text{m}$ thick and 1.2 mm long to reach full deflection is $\sim 7 \text{ V}$, which is much higher than the estimated value 0.16 V . We suggest the possible reason is the difference of the microstructural composition between the spin-on Nafion film and Nafion 117, i.e., the cluster radius, the distance between clusters, and the radius of the polymer chain. A more detailed explanation is given in [21]. A summary of the performance of the micro ICPF Nafion actuators is given in Table III.

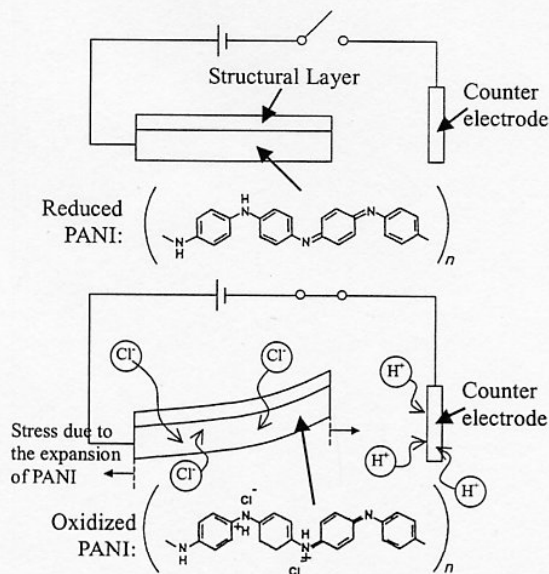


Fig. 11. Illustrations of PANI actuation principle.

V. PANI ACTUATORS

Polyaniline (PANI), a kind of conductive polymer, will undergo dimensional changes upon a reversible electrochemical oxidation-reduction (redox) reaction. This redox reaction is pH dependent, and can be activated by supplying abundant electrons. These properties make PANI one of the potential materials for making polymer actuators for underwater actuation. In acid, the polymer will be partially protonated. This reaction is reversible by de-protonation with base. As protonation means adding extra hydrogen ions (protons), PANI increases its size; while under de-protonation, it decreases its size. In a solution abundant of hydrogen ions (acid), protonation occurs; in a solution lack of hydrogen ions (alkaline), de-protonation occurs [23]. As PANI can undergoes protonation and de-protonation reversibly and repeatable, it can be used as an actuator under different pH medium. On the other hand, it is known that electrical potential can also drive this electrochemical reaction, with potential ranging from -0.4 V to 1.0 V. Recent research has shown that PANI can actuate upon electric field in wet condition with a gilded gold film [24], and in dry condition with a gel-like electrolyte [25].

In our lab, we use dichloroacetic acid (DCA) plus formic acid (FA) as the solvent, thus the PANI can be formed as solvent-casting films. The film thickness can be experimentally varied from 0.1 – 0.5 μm (spinning at 500 rpm to 4000 rpm). Using silver as the conductive and structural layer, the bi-layer strip bends toward the side of silver when acting as the anode, which indicates that PANI expands upon oxidation (see Fig. 11). This reaction is reversible with an opposite polarity.

A. Micro Fabrication PANI Actuators

We have also demonstrated some initial success in making PANI actuators in the micro scale using MEMS technology. We found that as a polymer, PANI cannot adhere well on normal metals and is insoluble to most of the acids. Thus, wet etching cannot be applied to pattern PANI. The PANI

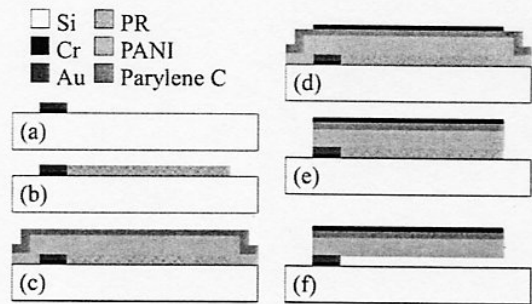


Fig. 12. PANI fabrication process. (a) Deposition and lift-off of conductive chromium/gold layer. (b) Deposition and pattern of sacrificial PR. (c) Spin-on PANI and coat Parylene. (d) Deposition and patterning of Chromium. (e) Plasma pattern Parylene/PANI. (f) Sacrificial release.

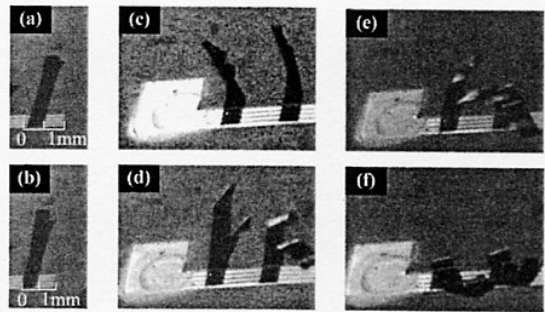


Fig. 13. PANI actuated in water. (a) Positive potential. (b) Negative potential. (c)–(f) are the time-sequenced pictures of PANI reacting with acid.

fabrication method is shown in Fig. 12, using photoresist as the sacrificial layer. Two sizes of prototype actuators were fabricated: 500 $\mu\text{m} \times 2.5$ mm, and 1000 $\mu\text{m} \times 5$ mm (with thickness of PANI/parylene/Cr film layers).

B. Experimental Results

The PANI actuators were tested in 0.5 M HCl with 2.5 V actuating potential. One electrode was connected to the pad and the other was dipped inside the solution. Connected to the positive terminal, the actuator lifted up [Fig. 13(a)–(b)]. Moreover, the actuator falls down due to its own weight when the power supply was cut.

When connected to the negative terminal, bubbles came out along the conductive path and no motion was observed. The bubbles were due to the hydrolysis effect of the aqueous solution. This reaction would cause the voltage potential to drop across the fluidic medium, so that the potential across PANI actuator has decreased dramatically, and hence, the redox reaction cannot be carried out along the PANI strip when a negative potential is used.

The actuating motion by changing the acidity of the fluidic medium is shown in Fig. 13(c)–(f), which is the ideal actuating motion for a PANI actuator undergoing full redox reaction.

The actuation force for the PANI actuator is estimated and provided in Table III. Since the fabrication process for micro PANI actuators is extremely complex, the experimental results described in this section is only preliminary. More detailed theoretical and experimental results will be published elsewhere shortly.

VI. CONCLUSION

Three different types of novel polymer-based MEMS underwater actuators were presented: 1) ionic conducting polymer films actuator, which actuates based on the stress gradient induced by ionic movement due to an applied electric field across the structural layer; 2) parylene thermal actuator, which actuates due to the induced stress gradient across a structure made of different layers of materials with different thermal expansion coefficients; 3) polyaniline actuator, which actuates due to its volumetric change caused by a reversible electrochemical oxidation-reduction reaction. All of these polymer materials are relatively new to the MEMS community and hence the majority of the research effort now is devoted to finding ways to fabricate them into movable structures using micro-lithographic techniques. We have developed various MEMS-compatible fabrication procedures to process these materials and have demonstrated that they can all be made into micro actuators that can be actuated underwater with large deflections using less than 7 V, and at a much lower power input than is required for conventional MEMS actuators. Our ongoing work is to design micro-mechanical structures that can be actuated under 2 V in water based the fabrication techniques we have developed.

REFERENCES

- [1] S. Yu and B. Nelson, "Microrobotic cell injection," in *Proc. IEEE Int. Conf. Robotics and Automation (ICRA 2001)*, Seoul, Korea, 2001, pp. 620-625.
- [2] S. Shoji and M. Esashi, "Microflow devices and systems," *J. Micromechan. Microeng.*, vol. 4, pp. 157-171, 1994.
- [3] G. Lin, C. J. Kim, S. Konishi, and H. Fujita, "Design, fabrication and testing of a C-shape actuator," in *Tech. Dig. Transducers '95*, Stockholm, Sweden, 1995, pp. 416-419.
- [4] M. Ataka, A. Omodaka, N. Takeshima, and H. Fujita, "Fabrication and operation of polyimide bimorph actuators for a ciliary motion system," *J. Microelectromech. Syst.*, vol. 2, no. 4, pp. 146-150, 1993.
- [5] E. W. H. Jager, O. Inganas, and I. Lundstrom, "Microrobots for micro-sized objects in aqueous media: Potential tools for single-cell manipulation," *Science*, vol. 288, pp. 2235-2238, 2000.
- [6] E. Smela, M. Kallenbach, and J. Holdenried, "Electrochemically driven polypyrrole bilayers for moving and positioning bulk micromachined silicon plates," *J. Microelectromech. Syst.*, vol. 8, no. 4, pp. 373-383, 1999.
- [7] H. Y. Chan and W. J. Li, "A thermally actuated polymer micro robotic gripper for manipulation of biological cells," in *Proc. IEEE Int. Conf. Robotics and Automation (ICRA 2003)*, Sept. 2003, pp. 288-293.
- [8] M. S. Weinberg, "Working equations for piezoelectric actuators and sensors," *J. Microelectromech. Syst.*, vol. 2, no. 4, pp. 529-533, 1999.
- [9] W. Riethmuller and W. Benecke, "Thermally excited silicon microrobots," *IEEE Trans. Electron Devices*, vol. 35, pp. 758-763, 1988.
- [10] Material Properties of Parylene Product from Cookson Electronics [Online]. Available: <http://www.scscookson.com/parylene/properties.cfm>
- [11] F. P. Ineropera and D. P. DeWitt, *Fundamentals of Heat and Mass Transfer*. New York: Wiley, 1981, pp. 85-86.
- [12] Material properties from Dupont Co.. [Online]. Available: http://www.dupont.com/fuelcells/pdf/extrusion_cast.pdf
- [13] Y. B. Cohen and S. P. Leary, "Electroactive polymers (EAP) characterization methods," in *Proc. SPIE Smart Structures and Materials*, vol. 3987, 2000, pp. 12-16.
- [14] E. Smela *et al.*, "Electrochemically driven polypyrrole bilayers for moving and positioning bulk micromachined silicon plates," *J. Microelectromechan. Syst.*, vol. 8, no. 4, pp. 373-383, 1999.
- [15] E. W. H. Jager *et al.*, "Microrobots for micron-size objects in aqueous media: Potential tools for single-cell manipulation," *Science*, vol. 288, pp. 2235-2238, 2000.
- [16] M. Y. F. Kwok, W. L. Zhou, W. J. Li, and Y. S. Xu, "Micro nafion actuators for cellular motion control and underwater manipulation," *Experimental Robot. VII: Series Lecture Notes Contr. Inform. Sci.*, vol. 271, pp. 471-480, 2001.
- [17] W. L. Zhou and W. J. Li, "MEMS-fabricated ICPF grippers for aqueous applications," in *Proc. 12th Int. Conf. Solid-State Sensors, Actuators, and Microsystems*, Boston, MA, June 2003, pp. 556-559.
- [18] P. G. D. Gennes, K. Okumura, and K. J. Kim, "Mechanoelectric effects in ionic gels," *Europhys. Lett.*, vol. 50, no. 4, pp. 513-18, 2000.
- [19] M. Shahinpoor, "Electro-mechanics of ionic-elastic beams as electrically controllable artificial muscles," in *Proc. SPIE*, vol. 3669, 1999, pp. 109-121.
- [20] K. R. S. Tadokoro, T. Takamori, M. Hattori, and K. Oguro, "Linear approximate dynamic model of an ICPF actuator," in *Proc. of IEEE Int. Conf. Robotics and Automation (ICRA 1996)*, 1996, pp. 219-225.
- [21] S. N. Nasser and J. Y. Li, "Electromechanical response of ionic polymer-metal composites," *J. Appl. Phys.*, vol. 87, no. 7, pp. 3321-3331, 2000.
- [22] W. L. Zhou and W. J. Li, "Micro ICPF actuators for aqueous sensing and manipulation," *Sensors and Actuators A: Physical*, Jan. 22, 2004, to be published.
- [23] H. S. Nalwa, *Handbook of Organic Conductive Molecules and Polymer Volume 3, Conductive Polymers: Spectroscopy and Physical Properties*. New York: Wiley, 1997, pp. 735-784.
- [24] W. Lu, E. Smela, and B. R. Mattes, "Electrochemical actuation of gilded polyaniline bilayers in aqueous acid solutions," *Smart Structures and Materials*, p. 505, 2001.
- [25] D. D. Rossi and A. Mazzoldi, "Linear fully dry polymer actuators," in *Proc. SPIE Conf. Electroactive Polymer Actuators and Devices*, vol. 3669, 1999, pp. 35-44.



Jennifer W. L. Zhou received the B.S degree in instrumentation technology and the M.S. degree in microelectronics from the Huazhong University of Science and Technology, China, in 1990 and 1995, respectively. She is currently working toward the Ph.D. degree at The Chinese University of Hong Kong.

She joined the Department of Electronic Science and Technology of Huazhong University of Science and Technology in 1995. Her research interests include fabrication, characterization, and applications

of MEMS sensors, actuators, transducers, and their systems.



Ho-Yin Chan received the B.S. degree in mechanical and automation engineering from The Chinese University of Hong Kong (CUHK) in 2001, where he is currently pursuing the M.S. degree in automation and computer-aided engineering.

His research interests include the development of micro-cellular gripper using MEMS technology and robot control and design.

Mr. Chan received the Best Conference Paper Award, with his supervisor, from IEEE ICRA 2003, for his work on micro parylene actuators.



Tony K. H. To received the B.S. degree in mechanical and automation engineering from The Chinese University of Hong Kong (CUHK) in 2001, where he is currently pursuing the M.S. degree in automation and computer-aided engineering.

He is a Graduate Research Assistant at the Center of Micro and Nano Systems Laboratory at CUHK. His research interests include MEMS fabrication, bio-MEMS and robot control and design.



King W. C. Lai received the B.E. degree in mechanical engineering and the M.Phil. degree from The Chinese University of Hong Kong (CUHK) in 2000 and 2002, respectively, where he is currently pursuing the Ph.D. degree.

His research interest is the development of micro cellular surgery tools using MEMS and Nanotechnology.



Wen J. Li (M'98) received the B.S. and M.S. degrees in aerospace engineering from the University of Southern California, Los Angeles, in 1987 and 1989, respectively, and the Ph.D. degree from University of California, Los Angeles, in 1997.

He has worked with The Aerospace Corporation, Silicon Microstructures Inc., and the NASA/CalTech Jet Propulsion Laboratory. He joined the Department of Automation and Computer-Aided Engineering, The Chinese University of Hong Kong (CUHK) in 1997. In the past six years he has published more

than 110 papers in international journals and conference proceedings on MEMS and nanotechnology-related work. He is serving as the Director of the Center for Micro and Nano Systems at CUHK and also as a Member of the Technical Committee on Nanorobotics and Nanomanufacturing of the IEEE Nanotechnology Council. His research interests are in micro/nano sensing and manipulations.

Dr. Li received the Silicon Microstructures Incorporated Employee Award and a NASA Technical Innovation Award during his tenure in the industry. He is also a Distinguished Overseas Scholar of the Chinese Academy of Sciences. He is a Member of ASME.